

Published in final edited form as:

*Nat Struct Mol Biol.* 2011 May ; 18(5): 571–576. doi:10.1038/nsmb.2044.

## Conformational changes in IgE contribute to its uniquely slow dissociation rate from receptor FcεRI

M.D. Holdom<sup>1,6</sup>, A.M. Davies<sup>1,6</sup>, J.E. Nettleship<sup>2,3</sup>, S.C. Bagby<sup>4,5</sup>, B. Dhaliwal<sup>1</sup>, E. Girardi<sup>1</sup>, J. Hunt<sup>1,5</sup>, H.J. Gould<sup>1</sup>, A.J. Beavil<sup>1</sup>, J.M. McDonnell<sup>1</sup>, R.J. Owens<sup>2,3</sup>, and B.J. Sutton<sup>1</sup>

<sup>1</sup>King's College London, Randall Division of Cell and Molecular Biophysics, New Hunt's House, Guy's Campus, London, SE1 1UL, UK; MRC & Asthma UK Centre in Allergic Mechanisms of Asthma, London, UK

<sup>2</sup>University of Oxford, The Oxford Protein Production Facility, Division of Structural Biology, Roosevelt Drive, Oxford, OX3 7BN, UK

<sup>3</sup>OPPF-UK, The Research Complex at Harwell, Rutherford Appleton Laboratory, Harwell Science & Innovation Centre, OX11 0FA, UK

<sup>4</sup>University of Oxford, Laboratory of Molecular Biophysics, Department of Biochemistry, South Parks Road, Oxford, OX1 3QU, UK

### Abstract

Of all the antibody classes, IgE displays a uniquely slow dissociation rate from, and high affinity for, its cell surface receptor FcεRI. The structural basis for these key determinants of IgE's ability to mediate allergic hypersensitivity is now revealed by the 3.4Å resolution crystal structure of human IgE-Fc (consisting of the Ce2, Ce3 and Ce4 domains) bound to the extracellular domains of the FcεRI α-chain. Comparison with free IgE-Fc (reported here at 1.9Å) shows that the antibody, which has a compact, bent structure prior to receptor engagement, becomes even more acutely bent in the complex. Thermodynamic analysis indicates that the interaction is entropically driven, which explains how the non-contacting Ce2 domains, in place of the flexible hinge region of IgG antibodies, contribute together with the conformational changes to IgE's unique binding properties.

The global incidence of allergic disease has increased markedly in recent years and continues to rise. Asthma currently affects 22.2 million people in North America and 5.4 million in the UK where the rate of incidence, especially in children, is among the highest in the world<sup>1</sup>. Anaphylactic reactions to foods such as nuts, virtually unknown thirty years ago, are now relatively common. The reason for this increase is debated, but these and other allergic conditions (rhinitis, eczema *etc.*) are all mediated by IgE, and the viability of

*Corresponding author:* Brian J. Sutton. King's College London, Randall Division of Cell and Molecular Biophysics, New Hunt's House, Guy's Campus, London, SE1 1UL, UK. Tel: 00 44 (0) 20 7848 6423. Fax: 00 44 (0) 20 7848 6410. brian.sutton@kcl.ac.uk.

<sup>5</sup>Current address: University of California, Department of Earth Science, Marine Science Institute, Webb Hall, Santa Barbara, CA 93106, USA (SCB); Novartis Horsham Research Centre, Wimbleshurst Road, Horsham, RH12 5AB, UK (JH)

<sup>6</sup>These authors contributed equally to this work

**AUTHOR CONTRIBUTIONS** MDH and AMD carried out the crystallographic analysis of the complex, and BD the crystallographic analysis of IgE-Fc; MDH, JEN, JH, AJB and RJO produced the proteins; SCB and JMM carried out the thermodynamic analysis; EG contributed to the analysis of the conformational changes; HJG, AJB and BJS planned and directed the project; MDH, AMD, JMM and BJS wrote the paper.

**Accession codes.** Atomic coordinates and structure factors have been deposited in the Protein Data Bank with entry codes 2WQR for IgE-Fc and 2Y7Q for the complex.

targeting its interaction with FcεRI therapeutically has been demonstrated by the recent success of the anti-IgE monoclonal antibody omalizumab in treating severe asthma<sup>2</sup>.

IgE binds to FcεRI through its Fc region, and it is this tight binding ( $K_A \approx 10^{10} \text{ M}^{-1}$ ) that sensitizes mast cells and basophils for immediate activation upon cross-linking by multivalent allergen<sup>3</sup>. The exceptionally slow dissociation rate ( $k_{off} \approx 10^{-5} \text{ s}^{-1}$ ), several orders of magnitude slower than that of IgG from any of its receptors<sup>4</sup>, contributes to the persistence of sensitization, and together with local IgE synthesis ensures that for allergic individuals the receptors in tissue are saturated with IgE<sup>5</sup>. The kinetics of IgE and IgE-Fc binding to FcεRI on cells, and to a soluble fragment consisting of the two extracellular domains of the α-chain, sFcεRIα, which are alone responsible for IgE-binding activity, have been studied extensively<sup>6-9</sup>. Particular interest has centered on the role of the Cε2 domains, which were shown to contribute to the slow dissociation rate<sup>10</sup>, by comparing the binding kinetics of the complete IgE-Fc (dimer Cε2-Cε3-Cε4 domains) with a sub-fragment lacking the Cε2 domains, here referred to as Fcε3-4. The Cε2 domains have no counterpart in IgG, all four subclasses of which have in their place hinge regions of various lengths and degrees of flexibility.

Early fluorescence resonance energy transfer (FRET) studies of labelled chimeric IgE indicated a more compact and bent structure than the extended, flexible Y-shaped IgG<sup>11</sup>, and later solution scattering studies of IgE-Fc were consistent with such a structure<sup>12</sup>. The crystal structure of IgE-Fc revealed for the first time the extent and nature of this bend<sup>13</sup>, made possible by the presence of the Cε2 domains. Surprisingly the molecule was found to be so acutely and asymmetrically bent, with the Cε2 domain pair folded back across the Cε3 domains, that one Cε2 domain even contacted the Cε4 domain of the other chain. The first view of the receptor interaction came from the structure of a complex between an Fcε3-4 fragment lacking the Cε2 domains, and sFcεRIα<sup>14</sup>. Both Cε3 domains were found to be involved, with a distinct sub-site on each domain, thus explaining the observed 1:1 stoichiometry despite the presence of two identical ε-chains. However, when compared with the unliganded IgE-Fc structure containing the Cε2 domains, only one of these two Cε3 sub-sites was found to be fully accessible, implying that conformational changes must occur, involving not only the Cε3 but also the Cε2 domains. We thus proposed an opening up of the bent structure<sup>13</sup> and involvement of the Cε2 domains<sup>10</sup> upon receptor engagement.

The structure of the human IgE-Fc/sFcεRIα complex reported here, together with that of free IgE-Fc at higher resolution, reveals the conformational changes that occur in both IgE and receptor upon binding, and shows how the slow dissociation rate is achieved despite the unexpected absence of any direct contact between the receptor and the Cε2 domains. Thermodynamic analysis of the interaction indicates how the non-contacting Cε2 domains nevertheless contribute to the unique receptor-binding properties of IgE. Knowledge of these structures and their conformational changes also suggests ways in which small molecules might allosterically prevent high-affinity binding; inhibition of protein/protein interactions such as this have hitherto been considered intractable<sup>15</sup>.

## RESULTS

### Structure of IgE-Fc bound to sFcεRIα

We determined the crystal structure of the complete IgE-Fc bound to sFcεRIα at 3.4 Å resolution, and also extended the resolution of the free IgE-Fc structure to 1.9 Å (see Methods and Table 1). Although crystallized under different conditions, the free IgE-Fc structure was essentially identical to that reported earlier at 2.6 Å<sup>13</sup>; however, features such as the carbohydrate and edge strands in the Cε2 domains (see below) were more clearly defined. The structure of the complex (Fig. 1 and Supplementary Video 1) shows that the

bound IgE molecule is oriented with its antigen-binding (Fab) arms pointing directly away from the cell membrane. Conformational changes occur in both the receptor and the C $\epsilon$ 2 and C $\epsilon$ 3 domains of IgE upon receptor engagement, but rather than an “unbending” of the molecule, IgE-Fc becomes *more* compact and bent, with no direct contact between the C $\epsilon$ 2 domains and receptor. This bend in the IgE molecule can be described in terms of the acute angle between the local two-fold axes of symmetry of the (C $\epsilon$ 2) $_2$  and (C $\epsilon$ 4) $_2$  domain pairs, which in free IgE-Fc is 62°, but in the complex is 54°. Despite the more compact structure, the C $\epsilon$ 3 domains move apart upon complex formation, allowing interaction at both sub-sites, designated 1 (in C $\epsilon$ 3A) and 2 (in C $\epsilon$ 3B) following previous nomenclature<sup>13,14</sup> (Fig. 1a). In free IgE-Fc only sub-site 2 (chain B) is fully accessible to receptor binding, and access to sub-site 1 is achieved by rotation of C $\epsilon$ 3A, taking both C $\epsilon$ 2 domains with it, relative to the C $\epsilon$ 4 domain pair, and away from C $\epsilon$ 3B. (Supplementary Fig. 1, and Videos 2 and 3).

This conformational change affects several inter-domain interactions within IgE-Fc. The extent of contact between C $\epsilon$ 2A and C $\epsilon$ 3B is reduced substantially (from 23 van der Waals contacts in free IgE-Fc down to only three in the complex), and contact between C $\epsilon$ 2B and C $\epsilon$ 4A is lost entirely upon receptor binding. Even though the molecule becomes increasingly bent, C $\epsilon$ 2B swings away from C $\epsilon$ 4A with the loss of two salt bridges (Glu270B–Lys497A; Lys302B–Glu472A) and associated hydrogen bonds. But as C $\epsilon$ 2B and C $\epsilon$ 4A move apart, C $\epsilon$ 2B moves closer to C $\epsilon$ 3B (Fig. 2) forming two potential hydrogen bonds (Asp271 in C $\epsilon$ 2B to the first and only ordered carbohydrate unit N-linked at Asn394 in C $\epsilon$ 3B; Fig. 2b) and van der Waals contacts (between Thr309 and Asn394, hidden behind Arg308 and the carbohydrate unit in the figure). These contacts prevent any further domain movement in this direction. This structural change however, presents an opportunity for allosteric inhibition. Occupation of this cleft between C $\epsilon$ 2B and C $\epsilon$ 3B in free IgE (Fig. 2a) by a small molecule could prevent its closure, thereby blocking the conformational change, access to sub-site 1 on C $\epsilon$ 3A, and consequently high-affinity receptor binding.

The relative orientation of the two extracellular domains of Fc $\epsilon$ RI $\alpha$  seen in the free state<sup>17,18</sup> is unchanged upon complex formation but, as observed in the earlier Fc $\epsilon$ 3-4/sFc $\epsilon$ RI $\alpha$  complex<sup>14</sup>, the loop and  $\beta$ -strand following the C strand in the  $\alpha$ 2 domain adopts a C' conformation alongside the C strand, rather than forming a D strand adjacent to the E strand on the other face of the domain. Intriguingly, a similar strand shift occurs in both C $\epsilon$ 2 domains of the IgE-Fc upon binding (Supplementary Fig. 2).

IgE contains carbohydrate chains N-linked to Asn394 in each C $\epsilon$ 3 domain, and these are high-mannose glycans, in contrast to the complex-type carbohydrate attached at the homologous location in the C $\gamma$ 2 domains of IgG<sup>19</sup>. The first five units (GlcNAc) $_2$ -(Man) $_3$  [(N-acetyl-glucosamine) $_2$ -(Mannose) $_3$ ] are well defined on both chains in the 1.9 Å resolution free IgE-Fc structure, but only the first GlcNAc unit is visible on each chain in the complex; the rest are disordered and mobile (Supplementary Fig. 3). The single ordered unit on C $\epsilon$ 3B is contacted by residues of C $\epsilon$ 2B following the conformational changes associated with receptor binding (Fig. 2b), and it may be that this contact affects the rest of the carbohydrate chain since in the Fc $\epsilon$ 3-4/sFc $\epsilon$ RI $\alpha$  complex<sup>14</sup> (determined at a similar resolution), three and six carbohydrate units can be seen on the two C $\epsilon$ 3 domains. No C $\epsilon$ 2 contact exists in the Fc $\epsilon$ 3-4 complex of course, and so disorder of the IgE-Fc carbohydrate may perhaps be a consequence of complex formation, and occur also in IgE.

### Nature of the IgE–receptor interface

Only the C $\epsilon$ 3 domains of IgE make direct contact with the receptor, through sub-sites 1 (C $\epsilon$ 3A) and 2 (C $\epsilon$ 3B) (Fig. 1a). The former contacts the C-C' loop region of the receptor  $\alpha$ 2 domain, while the latter interacts with the linker region between  $\alpha$ 1 and  $\alpha$ 2 and the B-C and F-G loops of  $\alpha$ 2, as seen in the earlier Fc $\epsilon$ 3-4/sFc $\epsilon$ RI $\alpha$  structure<sup>14</sup>. Given their effect upon

the binding kinetics, it is surprising that there is no direct contact between the Cε2 domains and the receptor. Based upon our previous report of an interaction in solution by NMR<sup>10</sup>, we suggested that “unbending” of the IgE might allow such contact<sup>13</sup>. In fact, the conformational change involving the Cε2 domains does enhance contact between the two proteins, but indirectly. Superposition of the IgE-Fc and Fcε3-4 receptor complex structures reveals that relative to the receptor, the two IgE fragments differ by a rotation of approximately 5° (Supplementary Fig. 3), leading to tighter contact and many more van der Waals interactions in the IgE-Fc complex. The cause of this difference in the angle of engagement appears to be the immediate proximity of the Cε2 domains, which affects the conformations of the linker from Cε2 leading into strand A and the adjacent B-C and F-G loops of Cε3. These are the very regions that present the contact residues, and thus the Cε2 domains play an indirect role in enhancing receptor binding.

Sub-site 1 on Cε3A includes two salt bridges between IgE-Fc and receptor (Arg334–Glu132; Asp362–Lys117; Fig. 3a) and the former forms a closer interaction and an additional hydrogen bond in the IgE-Fc complex compared with the Fcε3-4 complex. Tyr129 and Trp130 (Fig. 3a) also form closer and more extensive contacts in the IgE-Fc complex. (The electron density in this region is shown in Supplementary Fig. 4a). The dominant feature of sub-site 2 on Cε3B, and one that contributes a substantial fraction of the buried hydrophobic surface area, is the “proline sandwich”, in which Pro426 of Cε3B packs between Trp87 and Trp110 of the receptor α2 domain (Fig. 3b) - a feature conserved in IgG/FcγR interactions. However, there is a fascinating difference in the present structure: the orientation of the Trp87 side-chain in the IgE-Fc/receptor complex is “flipped” by precisely 180° compared with the Fcε3-4/receptor complex (and both of the known IgG1-Fc/FcγRIII complexes<sup>20,21</sup>) and its 6-membered ring, rather than the 5-membered ring, thus contributes additional van der Waals contacts to the proline sandwich (Fig. 3b). Both Trp87 rotamers have been observed in free receptor structures<sup>17,18</sup>, and IgE-Fc may initially “sample” both conformations, but the electron density (Supplementary Fig. 4b) indicates only a single conformation in the complex. Two other tryptophan residues in the receptor α2 domain (113 and 156) contribute to the hydrophobic interaction and also make tighter contacts with IgE-Fc than Fcε3-4; Trp156 for example makes 14 rather than 5 van der Waals contacts. Overall, the interaction is dominated by hydrophobic interactions and the total buried surface area of interaction is 1840 Å<sup>2</sup> (sub-site 1: 930 Å<sup>2</sup>, sub-site 2: 910 Å<sup>2</sup>).

### Thermodynamics of the interaction and role of Cε2 domains

The presence of the Cε2 domains thus enhances - indirectly - stabilization of the bound complex, and this is supported by published kinetic data showing that their effect is principally to decrease the dissociation rate<sup>10</sup>. We also investigated the thermodynamics of the interaction with and without the Cε2 domains, and revealed yet another striking difference that sheds further light on their role in the mechanism of binding. The temperature dependence of the binding kinetics and equilibrium binding affinities was determined by surface plasmon resonance (SPR) (Fig. 4), from which thermodynamic parameters (Table 2) were derived for IgE-Fc and Fcε3-4 binding to both wild-type receptor and a point mutant designed to assess the contribution of Trp87, part of the proline sandwich in sub-site 2 described above. The clear differences between the temperature dependences of the IgE-Fc and Fcε3-4 traces, and the gradients of the van't Hoff plots, indicate that the balance between the enthalpic and entropic contributions to the free energies of interaction depends upon whether the Cε2 domains are present or not. While Fcε3-4/sFcεRIα complex formation is enthalpically driven ( $\Delta H = -37.0$  kJ mol<sup>-1</sup>) with a small favorable entropic component ( $T\Delta S = +11.0$  kJ mol<sup>-1</sup>), IgE-Fc/sFcεRIα complex formation is strongly entropically driven ( $T\Delta S = +51.0$  kJ mol<sup>-1</sup>) with virtually no overall enthalpic component ( $\Delta H = +0.3$  kJ mol<sup>-1</sup>). Since the binding interfaces of both fragments with FcεRI are

generally similar, this marked difference in the thermodynamic parameters can only be due to the presence or absence of the C $\epsilon$ 2 domains.

The strongly hydrophobic nature of the IgE-Fc/Fc $\epsilon$ RI $\alpha$  interface would be expected to lead to a large and favorable (solvent) entropic contribution to the free energy of interaction, as observed with wild-type receptor. When the binding of IgE-Fc to the W87D receptor mutant was measured, the  $T\Delta S$  term fell from +51.0 kJ mol<sup>-1</sup> to +38.4 kJ mol<sup>-1</sup> (with an even larger reduction for Fc $\epsilon$ 3-4 binding), consistent with this interpretation. The disruption of this key hydrophobic interaction results in greatly destabilized complexes; the W87D receptor mutant with Fc $\epsilon$ 3-4 in particular has kinetic rate constants that are more typical of IgG-receptor interactions<sup>4</sup>, and demonstrates the contribution that a single amino-acid residue can make to an interaction. However, hydrophobicity differences cannot explain the effect of the C $\epsilon$ 2 domains on the thermodynamics of the interaction, which will be discussed below.

## DISCUSSION

The discovery that the bend in the IgE molecule is even more pronounced in the complex is consistent with the original FRET studies that reported increased rigidity of a chimeric murine IgE upon receptor binding<sup>11</sup>. This conformation orients IgE's Fab arms away from the cell surface (Fig. 1) and, although there is some uncertainty in the orientation of the two extracellular receptor domains, this might place structural constraints upon IgE's ability to recognize and be cross-linked by particular allergens and their epitopes. An acutely bent structure must also impose restrictions upon allergen recognition by the membrane-anchored form of IgE (mIgE) expressed on B cells, if the Fab arms are in that case oriented towards the cell surface. Recent crystal structures of allergen Fab complexes have provided some initial insights into this issue<sup>22-26</sup>: a particular feature of two of these complexes is the dimeric nature of the allergen<sup>24,25</sup>, which displays the epitopes in a defined (dyad-related) manner. Indeed, dimerization may be critical for allergens with a single epitope specificity to promote cross-linking<sup>24,25,27</sup>, and epitope location together with the orientation of the IgE Fab relative to each allergen monomer may determine whether or not it can be recognized by mIgE or trigger mast cells sensitized with receptor-bound IgE. A key question to answer is the degree of Fab flexibility relative to Fc in the IgE molecule, to bring together our structural understanding of IgE-Fc and Fab/allergen complexes; currently only limited information is available concerning the segmental flexibility of IgE by FRET<sup>11</sup> or EM<sup>28</sup> studies.

The adoption of this more acutely bent IgE structure does not lead to any direct receptor contact with either C $\epsilon$ 2 domain. How, therefore, do the C $\epsilon$ 2 domains influence the kinetics of the interaction? Their effect is clearly seen in the slower off-rates for IgE-Fc (Fc $\epsilon$ 2-4) compared with Fc $\epsilon$ 3-4 (Fig. 4), even more dramatically for W87D, and the markedly different temperature dependences and derived thermodynamic parameters (Table 2). IgE-Fc binding is exclusively driven by a large entropic component, in contrast to the enthalpically driven Fc $\epsilon$ 3-4; this provides a clue to the stabilizing contribution of the C $\epsilon$ 2 domains.

The C $\epsilon$ 3 domain in isolation adopts a partially unfolded "molten globule" state<sup>29,30</sup> and becomes more structured upon receptor binding<sup>30</sup>. In the context of IgE-Fc, C $\epsilon$ 3 is more sensitive to thermal denaturation than C $\epsilon$ 2<sup>31,32</sup> and becomes more resistant to thermal denaturation when receptor-bound<sup>32</sup>. This loss of conformational entropy of the two C $\epsilon$ 3 domains will be considerable for the Fc $\epsilon$ 3-4 fragment, which lacks any stabilizing interactions of the C $\epsilon$ 2 domains packing against them in the bent IgE structure; indeed the several crystal structures of Fc $\epsilon$ 3-4 reveal substantial conformational flexibility<sup>33,34</sup>. This large entropic penalty upon binding counteracts the favorable (solvent) entropic contribution



from the hydrophobic nature of the interaction, leading to the much smaller net entropic term for Fcε3-4 ( $T\Delta S = +11.0 \text{ kJ mol}^{-1}$ ) than for IgE-Fc ( $T\Delta S = +51.0 \text{ kJ mol}^{-1}$ ). This ordering of the Cε3 domains in Fcε3-4 upon receptor binding is reflected in the favorable enthalpy term ( $\Delta H = -37.0 \text{ kJ mol}^{-1}$ , cf.  $\Delta H = +0.3 \text{ kJ mol}^{-1}$  for IgE-Fc), as more stable intra-domain hydrogen bonds and optimal van der Waals interactions are formed; this is a typical example of entropy/enthalpy compensation. In summary, the Cε2 domains in IgE-Fc (and IgE) “pre-order” the Cε3 domains, thereby minimizing the loss of conformational entropy upon binding (or gain of entropy upon dissociation) for this intrinsically unstable domain. The full benefit of the hydrophobic interaction can thus be achieved.

The kinetic and thermodynamic parameters for IgE binding to FcεRIα are very similar to those of IgE-Fc (derived in the same way by SPR, data not shown), and thus the Cε2 domains play the same ordering role in the intact antibody. IgG has no counterpart to the Cε2 domains, only the flexible hinge region, and the thermodynamics of its binding to Fc receptors<sup>4</sup> is more like that of Fcε3-4, enthalpically driven and with lower affinities and faster dissociation rates. The unique binding properties of IgE - high affinity and slow dissociation rate - can thus be seen to result from a number of factors: a) the IgE/FcεRI interface contains a greater fraction of buried hydrophobic surface area than that of the structurally homologous IgG/FcγR interactions<sup>35</sup>, and other differences in detail between the interfaces may also contribute; b) the Cε2 domains are part of a conformational change in the IgE-Fc that involves movement of three of the six domains relative to the other three, making new inter-domain contacts while breaking others, whereas the conformational change in IgG-Fc involves only the loosely tethered Cγ2 domains moving apart; c) the presence of the Cε2 domains leads to a closer engagement with the receptor of the Cε3 domains in IgE-Fc (with the formation of a greater number of van der Waals interactions and hydrogen bonds compared with Fcε3-4); d) the Cε2 domains stabilize the interacting Cε3 domains and give rise to a bent and less flexible antibody molecule than IgG, thus reducing the entropic penalty of binding through these intrinsically less-ordered domains. All of these factors together contribute to creating a larger energy barrier against dissociation, and thus a slower off-rate for IgE compared with IgG. It is remarkable that the Cε2 domains, with no direct receptor contact, contribute so profoundly to the defining functional characteristics of the IgE molecule.

Knowledge of these structures and their conformational changes offers a basis for small molecule inhibitor design to target this extensive, high-affinity protein/protein interaction. Earlier studies with receptor-derived peptides<sup>36</sup> or IgE-Fc, including the intact Cε3 domain<sup>37</sup>, demonstrated inhibition by direct blocking with  $K_i$  values in the micromolar range, but none was developed into a small, non-peptide analogue. However, several locations can be identified in IgE-Fc at which the binding of a small molecule might prevent the conformational change, access to both sub-sites and the formation of a long-lived, stable complex. One example has already been highlighted (Fig. 2); a small molecule bound in the cleft between the Cε2B and Cε3B domains in free IgE could “lock” the antibody in a conformation incapable of fully engaging the receptor using both sub-sites. We previously determined the affinity for receptor binding to a single Cε3 domain in the context of an Fcε3-4 fragment, and found that this was reduced by at least three orders of magnitude ( $K_A \approx 106 \text{ M}^{-1}$ ), due principally to a faster off-rate<sup>38</sup>. We also know that an attenuation of two orders of magnitude in the affinity of IgE binding, again with a faster off-rate, leads to a 75% reduction of passive cutaneous anaphylaxis *in vivo* in a transgenic mouse model<sup>39</sup>, and thus partial inhibition can achieve a physiological effect. An allosteric approach may be the key to inhibiting this protein/protein interaction, heralding a new generation of anti-IgE therapeutics for intervention in allergic disease.

## METHODS

### Protein expression and purification

The human IgE-Fc (Fc $\epsilon$ 2-4) construct has been reported previously<sup>13</sup> and, as for Fc $\epsilon$ 3-4, was expressed in mammalian NS0 cells and purified as described<sup>7</sup>. The sFc $\epsilon$ RI $\alpha$  construct coding for residues 1–176 of a triple glycosylation mutant (N74A, N135A, T142A)<sup>14</sup> with C-terminal Lys-His<sub>6</sub> tag was amplified and subcloned into a pHLSec vector<sup>40</sup>, produced by transient transfection in HEK293S cells, which restrict protein glycosylation to (GlcNAc)<sub>2</sub>-(Man)<sub>5</sub>, and purified as previously described<sup>40</sup>. The complex was formed by mixing IgE-Fc and sFc $\epsilon$ RI $\alpha$  in a 1:1 molar ratio at 4° C overnight, purified by size exclusion (Superdex 200 column), eluted in 20 mM Tris pH 7.5, 200 mM NaCl, concentrated by centrifugation at 4° C ( $A_{280}$  = 20) and stored at 4° C.

### Crystallization

The complex was crystallized by vapor diffusion. The reservoir contained 95  $\mu$ l of 2.8 M sodium acetate, pH 7.0, and the drop consisted of 100 nl of the concentrated protein solution ( $A_{280}$  = 20) with an equal volume of reservoir. A single crystal suitable for data collection, measuring  $\sim$ 110  $\times$  40  $\times$  30  $\mu$ m, grew after two months at 21° C. IgE-Fc was buffer exchanged to 25 mM Tris-HCl pH 7.5, 20 mM NaCl and 0.05% (w/v) sodium azide, and concentrated to 2 mg ml<sup>-1</sup>. Crystals were grown by vapor diffusion, with a 500  $\mu$ l reservoir of 100 mM Tris-HCl, pH 8.5, 14% (w/v) PEG 8000 and 200 mM lithium sulphate, and a drop containing 1  $\mu$ l of protein solution and 0.5  $\mu$ l of the reservoir solution. Crystals, typically  $\sim$ 50  $\times$  50  $\times$  10  $\mu$ m, grew after 1–2 weeks at 18° C.

### Data collection, structure determination and refinement

One crystal of the complex was cryoprotected in perfluoropolyether oil and flash-cooled to 100 K. X-ray data were collected at beamline ID29 at the European Synchrotron Radiation Facility, Grenoble, France, integrated with MOSFLM<sup>41</sup> and further processed with the CCP4 program suite<sup>42</sup>. The space group was  $P2_12_12_1$  and the Matthews coefficient indicated one complex (one sFc $\epsilon$ RI $\alpha$  and one IgE-Fc dimer) in the asymmetric unit with 48% solvent content. The structure was solved using MOLREP<sup>43</sup> from the CCP4 suite. Fc $\epsilon$ 3-4 and sFc $\epsilon$ RI $\alpha$  from the Fc $\epsilon$ 3-4/sFc $\epsilon$ RI $\alpha$  complex structure<sup>14</sup> (PDB code 1F6A) and (C $\epsilon$ 2)<sub>2</sub> from IgE-Fc<sup>13</sup> (PDB code 1O0V) were used as search models for the first stage of molecular replacement (MR). Each refinement round was alternated with one round of manual model building with *Coot*<sup>44</sup>. Early rounds were performed with CNS<sup>45</sup>, and the sFc $\epsilon$ RI $\alpha$  chain and each of the six Fc domains were refined as rigid units with one overall *B*-factor per domain. Electron density maps were calculated omitting each domain turn to check for and prevent any bias. Later rounds were performed with PHENIX<sup>46</sup>. NCS restraints were applied for C $\epsilon$ 3 and C $\epsilon$ 4 domain residues with grouped *B*-factor refinement (one per residue). Carbohydrate atoms were subsequently incorporated into the structure, but no water or other small molecules. The coordinate error was 0.47 Å, and the final model analyzed with SFCHECK<sup>47</sup> and MolProbity<sup>48</sup>; Ramachandran analysis revealed 90.9% (favored) and 97.7% (allowed).

X-ray data for free IgE-Fc were collected at the Diamond Light Source, beamline I04, from a crystal flash-cooled to 100 K in 100 mM Tris-HCl, pH 8.5, 30% (w/v) PEG 8000 and 200 mM lithium sulfate. The structure was solved by MR using the previously reported structure as a search model<sup>13</sup>. Although the crystallization conditions are different, the space groups are the same and cell dimensions differ only slightly. Data processing was carried out using HKL2000<sup>49</sup>, and a MR solution was found using MOLREP<sup>43</sup>. Iterative cycles of refinement using PHENIX<sup>46</sup> (including bulk-solvent scaling, conjugate gradient minimization, individual *B*-factor refinement and TLS refinement) alternated with manual model building

with  $Cool^{44}$ . To minimize bias, the model was built into  $2F_{obs}-F_{calc}$  composite omit,  $2F_{obs}-F_{calc}$  and  $F_{obs}-F_{calc}$  electron density maps. TLS groups were generated using the TLSMD web server<sup>50</sup>. Polyethylene glycol molecules were identified using AFITT<sup>51</sup>. The coordinate error was 0.26 Å, and the final model evaluated with MolProbity<sup>48</sup>; Ramachandran analysis revealed 97.0% (favored) and 100% (allowed).

Molecular superpositions were performed using CCP4MG<sup>42</sup>, and interfaces determined using the Protein Interfaces Surfaces and Assemblies (PISA) service at the European Bioinformatics Institute<sup>52</sup>. Buried surface areas were calculated using CNS<sup>45</sup>. Contact residues were defined using CCP4 CONTACT<sup>42</sup> (with a cut-off of 4.0 Å) and confirmed by manual inspection. Secondary structures were assigned using KSDSSP implemented in CHIMERA<sup>53</sup>. Protein domain movements were analyzed with DynDom<sup>54,55</sup> using 1O0V, 1FP5, 1F6A (PDB codes) and the structures described here. Planar and dihedral angles were measured by defining vectors corresponding to the local two-fold axes of the (Ce4)<sub>2</sub> and (Ce2)<sub>2</sub> domain pairs and calculating the dot product between them or by direct measurement in PyMOL<sup>56</sup>. Figures were produced with PyMOL<sup>56</sup> and videos created using the eMovie plugin<sup>57</sup> for PyMOL. Morphs were created using RigiMOL in iPyMOL.

### Surface plasmon resonance analysis

Experiments were performed on a Biacore 2000 instrument (GE Healthcare, Uppsala, Sweden). Specific binding surfaces were prepared by coupling sFcεRIα through carbohydrate to a CM5 sensor chip *via* aldehydes as described previously<sup>9</sup>. Coupling density was limited to <400 RU. Samples of IgE, Fcε2-4 (IgE-Fc) or Fcε3-4 were dialyzed into HBS (10 mM HEPES pH 7.4, 150 mM NaCl, 3.4 mM EDTA, 0.01% (v/v) Surfactant P-20) and injected over the sensor chip at a flow rate of 25 μl min<sup>-1</sup> at concentrations of 125, 62.5, 31.3, 15.6, 7.7 and 3.9 nM. Each data set was collected at 10, 15, 20, 25 and 30 °C. Analyte concentrations were injected in duplicate, a titration series of “low-to-high” analyte concentration followed by a “high-to-low” series. A two minute association phase was followed by a 15 minute dissociation phase. The sensor surface was regenerated by three 60 second pulses of 0.2 M glycine-HCl, pH 2.5. Standard double-referencing data subtraction methods were applied<sup>58</sup> prior to evaluation of rate constants and equilibrium binding. Association and dissociation curves were fitted using a biphasic interaction model, as described previously<sup>8</sup>. Data were analyzed using curve fitting software from Microcal Origin (OriginLab, Northampton, MA, USA).

### Supplementary Material

Refer to Web version on PubMed Central for supplementary material.

### Acknowledgments

We thank Nahid Rahman for assistance with receptor protein production (Oxford Protein Production Facility), Tom Walter for technical advice on crystallization of the complex, and Karl Harlos and Christian Siebold (Division of Structural Biology, Wellcome Trust Centre for Human Genetics, Oxford) for X-ray data collection of the complex, together with beamline support staff at ESRF. This work was also carried out with the support of the Diamond Light Source. The work was funded by Asthma UK and the Medical Research Council (UK).

### REFERENCES

1. Asher MI, et al. Worldwide time trends in the prevalence of symptoms of asthma, allergic rhinoconjunctivitis, and eczema in childhood: ISAAC Phases One and Three repeat multicountry cross-sectional surveys. *Lancet*. 2006; 368:733–743. [PubMed: 16935684]
2. Holgate S, et al. The use of omalizumab in the treatment of severe allergic asthma: A clinical experience update. *Respir. Med.* 2009; 103:1098–1113. [PubMed: 19362459]



3. Gould HJ, Sutton BJ. IgE in allergy and asthma today. *Nature Rev. Immunol.* 2008; 8:205–217. [PubMed: 18301424]
4. Maenaka K, van der Merwe PA, Stuart DI, Jones EY, Sondermann P. The human low affinity Fc $\gamma$  receptors IIa, IIb and III bind IgG with fast kinetics and distinct thermodynamic properties. *J. Biol. Chem.* 2001; 276:44898–44904. [PubMed: 11544262]
5. Gould HJ, et al. The biology of IgE and the basis of allergic disease. *Ann. Rev. Immunol.* 2003; 21:579–628. [PubMed: 12500981]
6. Basu M, et al. Purification and characterization of human recombinant IgE-Fc fragments that bind to the human high affinity IgE receptor. *J. Biol. Chem.* 1993; 268:13118–13127. [PubMed: 7685756]
7. Young RJ, et al. Secretion of recombinant human IgE-Fc by mammalian cells and biological activity of glycosylation site mutants. *Protein Eng.* 1995; 8:193–199. [PubMed: 7543206]
8. Cook JPD, et al. Identification of contact residues in the IgE binding site of human Fc $\epsilon$ RI $\alpha$ . *Biochemistry.* 1997; 36:15579–15588. [PubMed: 9398286]
9. Henry AJ, et al. Participation of the N-terminal region of Ce3 in the binding of human IgE to its high affinity receptor Fc $\epsilon$ RI. *Biochemistry.* 1997; 36:15568–15578. [PubMed: 9398285]
10. McDonnell JM, et al. The structure of the IgE Ce2 domain and its role in stabilizing the complex with its high-affinity receptor Fc $\epsilon$ RI. *Nature Struct. Biology.* 2001; 8:437–441.
11. Zheng Y, Shopes B, Holowka D, Baird B. Dynamic conformations compared for IgE and IgG1 in solution and bound to receptors. *Biochemistry.* 1992; 31:7446–7456. [PubMed: 1387320]
12. Beavil AJ, Young RJ, Sutton BJ, Perkins SJ. Bent domain structure of recombinant human IgE-Fc in solution by X-ray and neutron scattering in conjunction with an automated curve fitting procedure. *Biochemistry.* 1995; 34:14449–14461. [PubMed: 7578050]
13. Wan T, et al. The crystal structure of IgE Fc reveals an asymmetrically bent conformation. *Nature Immunol.* 2002; 3:681–686. [PubMed: 12068291]
14. Garman S, Wurzburg B, Tarchevskava S, Kinet J-P, Jardetzky T. Structure of the Fc fragment of human IgE bound to its high-affinity receptor Fc $\epsilon$ RI $\alpha$ . *Nature.* 2000; 406:259–266. [PubMed: 10917520]
15. Whitty A, Kumaravel G. Between a rock and a hard place. *Nature Chem. Biol.* 2006; 3:112–118. [PubMed: 16484997]
16. Weiss MS. Global indicators of X-ray data quality. *J. Appl. Cryst.* 2001; 34:130–135.
17. Garman SC, Kinet J-P, Jardetzky TS. Crystal structure of the human high-affinity IgE receptor. *Cell.* 1998; 95:951–961. [PubMed: 9875849]
18. Garman SC, Sechi S, Kinet J-P, Jardetzky TS. The analysis of the human high affinity IgE receptor Fc $\epsilon$ RI $\alpha$  from multiple crystal forms. *J. Mol. Biol.* 2001; 311:1049–1062. [PubMed: 11531339]
19. Arnold JN, et al. The glycosylation of human serum IgD and IgE and the accessibility of identified oligomannose structures for interaction with mannan-binding lectin. *J. Immunol.* 2004; 173:6831–6840. [PubMed: 15557177]
20. Sondermann P, Huber R, Oosthuizen V, Jacob U. The 3.2Å crystal structure of the human IgG1 Fc fragment-Fc $\gamma$ RIII complex. *Nature.* 2000; 406:267–273. [PubMed: 10917521]
21. Radaev S, Motyka S, Fridman W-H, Sautes-Fridman C, Sun P. The structure of a human type III Fc $\gamma$  receptor in complex with Fc. *J. Biol. Chem.* 2001; 276:16469–16477. [PubMed: 11297532]
22. Mirza O, et al. Dominant epitopes and allergic cross-reactivity: complex formation between a Fab fragment of a monoclonal murine IgG antibody and the major allergen from birch pollen Bet v 1. *J. Immunol.* 2000; 165:331–338. [PubMed: 10861069]
23. Padavattan S, et al. Identification of a B-cell epitope of hyaluronidase, a major bee venom allergen, from its crystal structure in complex with a specific Fab. *J. Mol. Biol.* 2007; 368:742–752. [PubMed: 17374540]
24. Niemi M, et al. Molecular interactions between a recombinant IgE antibody and the  $\beta$ -lactoglobulin allergen. *Structure.* 2007; 15:1413–1421. [PubMed: 17997967]
25. Li M, et al. Crystal structure of a dimerized cockroach allergen Bla g 2 complexed with a monoclonal antibody. *J. Biol. Chem.* 2008; 283:22806–22814. [PubMed: 18519566]

26. Padavattan S, et al. High-affinity recognition of a conformational epitope of the major respiratory allergen Phl p 2 as revealed by X-ray crystallography. *J. Immunol.* 2009; 182:2141–2151. [PubMed: 19201867]
27. Rouvinen J, et al. Transient dimers of allergens. *PLoS ONE.* 2010; 5:1–9.
28. Roux KH, Strelets L, Brekke OH, Sandlie I, Michaelsen TE. Comparisons of the ability of human IgG3 mutants, IgM, IgE, and IgA2, to form small immune complexes: a role for flexibility and geometry. *J. Immunol.* 2001; 161:4083–4090. [PubMed: 9780179]
29. Henry AJ, McDonnell JM, Ghirlando R, Sutton BJ, Gould HJ. Conformation of the isolated Ce3 domain of IgE and its complex with the high-affinity receptor, FcεRI. *Biochemistry.* 2000; 39:7406–7413. [PubMed: 10858288]
30. Price NE, Price NC, Kelly SM, McDonnell JM. The key role of protein flexibility in modulating IgE interactions. *J. Biol. Chem.* 2005; 280:2324–2330. [PubMed: 15520005]
31. Dorrington KJ, Bennich H. Thermally induced structural changes in immunoglobulin E. *J. Biol. Chem.* 1973; 248:8378–8384. [PubMed: 4128478]
32. Demarest SJ, et al. An intermediate pH unfolding transition abrogates the ability of IgE to interact with its high affinity receptor FcεRIα. *J. Biol. Chem.* 2006; 281:30755–30767. [PubMed: 16905745]
33. Wurzburg BA, Garman SC, Jardetzky TS. Structure of the human IgE-Fc Ce3-Ce4 reveals conformational flexibility in the antibody effector domains. *Immunity.* 2000; 13:375–385. [PubMed: 11021535]
34. Wurzburg BA, Jardetzky TS. Conformational flexibility in immunoglobulin E-Fc<sub>3-4</sub> revealed in multiple crystal forms. *J. Mol. Biol.* 2009; 393:176–190. [PubMed: 19682998]
35. Sondermann P, Kaiser J, Jacob U. Molecular basis for immune complex recognition: a comparison of Fc-receptor structures. *J. Mol. Biol.* 2001; 309:737–749. [PubMed: 11397093]
36. McDonnell JM, et al. Structure based design and characterization of peptides that inhibit IgE binding to its high-affinity receptor. *Nature Struct. Biol.* 1996; 3:419–426. [PubMed: 8612071]
37. Vangelista L, et al. The immunoglobulin-like modules Ce3 and α2 are the minimal units necessary for human IgE-FcεRI interaction. *J. Clin. Invest.* 1999; 103:1571–1578. [PubMed: 10359566]
38. Hunt J, et al. Disulphide linkage controls the affinity and stoichiometry of IgE Fcε3-4 binding to FcεRI. *J. Biol. Chem.* 2005; 280:16808–16814. [PubMed: 15743766]
39. Hunt J, et al. Attenuation of IgE affinity for FcεRI radically reduces the allergic response *in vitro* and *in vivo*. *J. Biol. Chem.* 2008; 283:29882–29887. [PubMed: 18703499]
40. Nettleship JE, Rahman-Huq N, Owens RJ. The production of glycoproteins by transient expression in mammalian cells. *Methods Mol. Biol.* 2009; 498:245–263. [PubMed: 18988030]
41. Leslie AGW. Recent changes to the MOSFLM package for processing film and image plate data. *Joint CCP4 + ESF-EAMCB Newsletter on Protein Crystallography.* 1992; (No. 26)
42. Collaborative Computational Project, Number 4. The CCP4 suite: programs for protein crystallography. *Acta Crystallogr.* 1994; D50:760–763.
43. Vagin A, Teplyakov A. MOLREP: an automated program for molecular replacement. *J. Appl. Cryst.* 1997; 30:1022–1025.
44. Emsley P, Cowtan K. *Coot*: model-building tools for molecular graphics. *Acta Crystallogr.* 2004; D60:2126–2132.
45. Brünger AT, et al. Crystallography & NMR System: A new software suite for macromolecular structure determination. *Acta Crystallogr.* 1998; D54:905–921.
46. Afonine PV, Grosse-Kunstleve RW, Adams PD. The Phenix refinement framework. *CCP4 Newsletter.* 2005; (No. 42) contribution 8.
47. Vaguine AA, Richelle J, Wodak SJ. SFCHECK: a unified set of procedures for evaluating the quality of macromolecular structure-factor data and their agreement with the atomic model. *Acta Crystallogr.* 1999; D55:191–205.
48. Davis IW, et al. MolProbity: all-atom contacts and structure validation for proteins and nucleic acids. *Nucl. Acids Res.* 2007; 35:W375–W383. [PubMed: 17452350]
49. Otwinowski Z, Minor W. Processing of X-ray diffraction data collected in oscillation mode. *Methods Enzymol.* 1997; 276:307–326.

50. Painter J, Merritt EA. *TLSMD* web server for the generation of multi-group TLS models. *J. Appl. Cryst.* 2006; 39:109–111.
51. Wlodek S, Skillman AG, Nicholls A. Automated ligand placement and refinement with a combined force field and shape potential. *Acta Cryst.* 2006; D62:741–749.
52. Krissinel E, Henrick K. Inference of macromolecular assemblies from crystalline state. *J. Mol. Biol.* 2007; 372:774–797. [PubMed: 17681537]
53. Pettersen EF, et al. UCSF Chimera - A visualization system for exploratory research and analysis. *J. Comput. Chem.* 2004; 25:1605–1612. [PubMed: 15264254]
54. Hayward S, Berendsen JC. Systematic analysis of domain motions in proteins from conformational change; new research on citrate synthase and T4 lysozyme. *Proteins.* 1998; 30:144–154. [PubMed: 9489922]
55. Hayward S, Lee RA. Improvements in the analysis of domain motions in proteins from conformational change: DynDom version 1.50. *J. Mol. Graph. Model.* 2002; 21:181–183. [PubMed: 12463636]
56. DeLano, WL. *The PyMOL molecular graphics system.* DeLano Scientific; San Carlos, CA: 2002.
57. Hodis E, Schreiber G, Rother K, Sussman JL. eMovie: a storyboard-based tool for making molecular movies. *Trends in Biochem. Sci.* 2007; 32:199–204. [PubMed: 17448663]
58. Myszka DG. Improving biosensor analysis. *J. Molec. Recognition.* 1999; 12:279–284.

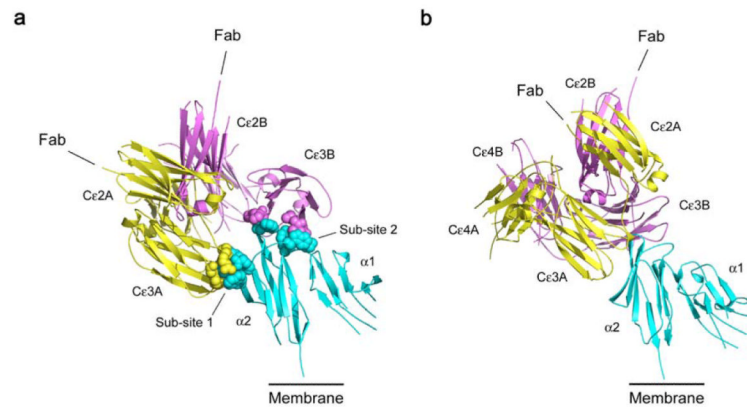


**Figure 1.**

Overall structure of the IgE-Fc/sFcεRIα complex, in two approximately orthogonal views. sFcεRIα is colored in blue, IgE-Fc chain A in yellow and chain B in purple. a) The extensive interface with two distinct sub-sites, one on each Cε3 domain, is indicated with a space-filled representation of the interacting side-chains. The Cε4 domains are hidden in this orientation. b) The acute bend, with the pair of Cε2 domains packed against the Cε3 and Cε4 domains, can be seen clearly. The connections to the Fab regions are indicated, and the bend in the IgE molecule ensures that they are oriented away from the membrane (see also Supplementary Video 1).

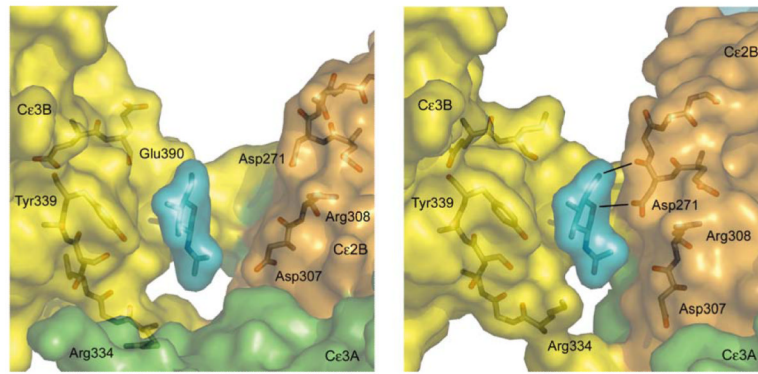


**Figure 2.**

Closure of an inter-domain cleft in IgE-Fc upon receptor binding. a) In the free IgE-Fc structure there is a cleft between the first N-acetylglucosamine carbohydrate unit (blue), N-linked to Asn394 (behind) in Cε3B (yellow), and residues Asp271 and Asp307 in Cε2B (orange). b) In the complex, the movement of Cε3A (green), Cε2B (orange) and Cε2A (not shown) as a rigid unit relative to Cε3B (yellow) and the Cε4 domains (not shown) closes the cleft, and Asp271 and carbohydrate make contact, with the formation of two potential H-bonds (black lines). Both figures are centered on the first N-acetylglucosamine unit. For clarity, other carbohydrate residues are not shown for the unbound form (panel a); all carbohydrate units except for the first N-acetylglucosamine were disordered in the complex (panel b).



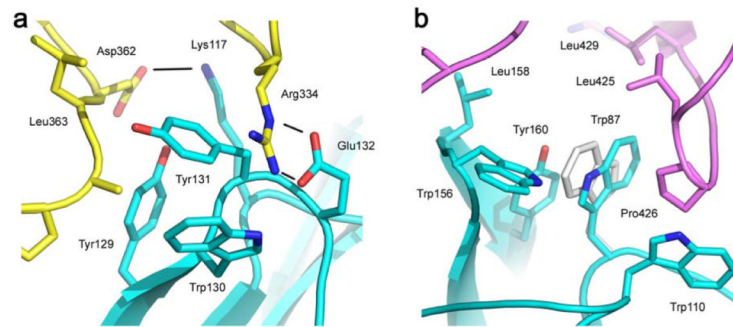


**Figure 3.** Interactions at the two sub-sites. a) Two salt bridges (Arg334–Glu132; Asp362–Lys117) with three hydrogen bonds (black lines) between residues of the Cε3A domain of IgE-Fc (yellow) and the receptor (blue) contribute to sub-site 1. b) The “proline sandwich” at sub-site 2, with Pro426 in the Cε3B domain of IgE-Fc (purple) packed between Trp87 and Trp110 of the receptor (blue). The alternative orientation of Trp87 observed in the Fcε3-4/sFcεRIα complex (light grey) can be seen to make fewer contacts and a weaker interaction with Pro426.

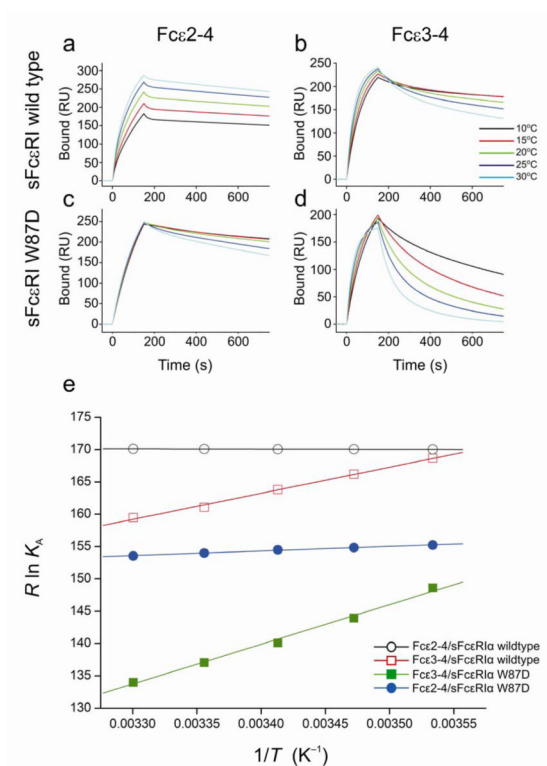


**Figure 4.** Thermodynamics of the IgE/FcεRI interaction. SPR sensorgrams of Fcε2-4 (IgE-Fc) and Fcε3-4 binding to immobilized sFcεRIα wildtype (a & b), and to immobilized sFcεRIα W87D (c & d), over a range of temperatures. A series of analyte concentrations were tested; sensorgrams for a single concentration point (125 nM) are shown for each temperature (see Supplementary Figs. 5 and 6 for full range of concentration data). (e) The van't Hoff plot illustrates the temperature dependence of the equilibrium binding affinities for Fcε2-4/sFcεRIα wildtype, Fcε2-4/sFcεRIα W87D, Fcε3-4/sFcεRIα wildtype, and Fcε3-4/sFcεRIα W87D. The fits for both Fcε2-4 interactions are linear ( $R > 0.99$ ), whereas the Fcε3-4 interactions show small deviations from linearity ( $R = 0.96-0.98$ ), consistent with a minor contribution from  $\Delta C_p$ . The derived thermodynamic parameters are summarized in Table 2.

Table 1

## Data collection and refinement statistics

	IgE-Fc/sFceRIa	IgE-Fc
<b>Data collection</b>		
Space group	$P2_12_12_1$	$P2_12_12$
Cell dimensions		
$a, b, c$ (Å)	99.49, 103.34, 110.12	130.50, 75.28, 79.14
Resolution (Å)	3.4 (3.49 – 3.40)	1.9 (1.97 – 1.90)
$R_{\text{merge}}$	0.112 (0.522) <sup>a</sup>	0.074 (0.533)
$I / \sigma I$	8.5 (1.6)	26.3 (2.9)
Completeness (%)	99.9 (99.9)	99.9 (100)
Redundancy	5.9 (6.1)	7.3 (7.4)
<b>Refinement</b>		
Resolution (Å)	37 – 3.4	36 – 1.9
No. reflections	16,204 (1,174)	62,035 (6,147)
$R_{\text{work}} / R_{\text{free}}$	0.245/0.292	0.193/0.234
No. atoms		
Protein	5,263	5,017
Non-protein	92 <sup>b</sup>	175 <sup>c</sup>
Water	0	533
$B$ -factors (Å <sup>2</sup> )		
Protein	77	48
Non-protein	76 <sup>b</sup>	77 <sup>c</sup>
Water	-	45
R.m.s. deviations		
Bond lengths (Å)	0.006	0.005
Bond angles (°)	1.104	1.001

Values in parentheses are for highest-resolution shell.

Data for each structure were collected from a single crystal.

<sup>a</sup> $R_{\text{pim}}$  precision-indicating  $R_{\text{merge}}$  <sup>16</sup>.

<sup>b</sup>Carbohydrate.

<sup>c</sup>Carbohydrate,  $\text{SO}_4^{2-}$ , 2-amino-2-hydroxymethyl-propane-1,3-diol (Tris), polyethylene glycol (PEG).

**Table 2**

Comparative thermodynamics of the interaction of sFcεRIα (wild-type and W87D mutant) with IgE-Fc and Fcε3-4 (derived from the data presented in Fig. 4)

	$\Delta H$ (kJ mol <sup>-1</sup> )	$T\Delta S$ (kJ mol <sup>-1</sup> )	$\Delta G$ (kJ mol <sup>-1</sup> )
<b>IgE-Fc (Fcε2-4)</b>			
sFcεRIα WT	0.3	51.0	-50.7
sFcεRIα W87D	-7.5	38.4	-45.9
<b>Fcε3-4</b>			
sFcεRIα WT	-37.0	11.0	-48.0
sFcεRIα W87D	-63.6	-22.6	-41.0